

# Toward Manipulating Quantum Information with Atomic Ensembles

M.D.Lukin<sup>1</sup>, A. André<sup>1</sup>, M. D. Eisaman<sup>1</sup>, M. Hohensee<sup>1</sup>, D. F. Phillips<sup>2</sup>,  
C. H. van der Wal<sup>1,2</sup>, R. L. Walsworth<sup>1,2</sup>, A. S. Zibrov<sup>1,2,3</sup>

<sup>1</sup>*Department of Physics, Harvard University, Cambridge, MA, 02138*

<sup>2</sup>*Harvard-Smithsonian Center for Astrophysics, Cambridge, MA, 02138*

<sup>3</sup>*P. N. Lebedev Institute of Physics, RAS, Leninsky pr. 53, Moscow, 117924*

## Abstract

We review several ideas for manipulation of quantum information using atomic ensembles and photons and describe some preliminary experiments toward their implementation. In particular, we review a technique that allows for robust transfer of quantum states between light fields and metastable states of matter. Next we discuss the use of Raman scattering to produce robust entanglement of atomic ensembles via realistic (i.e., absorbing) channels. Finally, we present preliminary experimental results related to the implementation of entanglement via Raman scattering. Specifically, we present experimental studies of the intensity fluctuations in resonantly enhanced Raman scattering from a warm <sup>85</sup>Rb vapor cell under conditions of EIT. A crossover between the Bose-Einstein and Poisson statistics of Raman light is observed and it is shown that the noise properties of Raman fields can be mirrored in transmitted pump beams.

## 1 Introduction: Quantum Memory for Light

Photons are the fastest and simplest carriers of quantum information, but their main strength is also their weakness: they are difficult to localize and store. It appears that an ideal solution would be to store and process quantum information in matter that forms the nodes of a quantum network, and to communicate between these nodes using photons [1]. Atoms, for example, represent reliable and long-lived storage and processing units. In this section, we review a technique that potentially allows for an ideal transfer of quantum states between light fields and metastable states of matter. The technique uses electromagnetically induced transparency (EIT) [2, 3] to map quantum states of photons into coherently driven atomic media by adiabatically reducing the group velocity of propagating pulses to zero, resulting in a coherently controlled absorption process.

EIT is a technique that can be used to make a resonant, opaque medium transparent by means of quantum interference. Consider the situation in which the atoms have a pair of lower energy metastable states ( $|g\rangle$  and  $|s\rangle$  in Fig. 1a). In order to modify the propagation of a “signal” light field (gray arrow) that couples the ground state  $|g\rangle$  to an electronically excited state  $|e\rangle$ , one can apply a second “control” field that is near resonance with the transition  $|e\rangle \rightarrow |s\rangle$  (black arrow). The combined effect of these two fields is to stimulate the atoms into a so-called dark superposition of the states  $|g\rangle$  and  $|s\rangle$ . In such a case, the two possible pathways in which light can be absorbed by atoms ( $|g\rangle \rightarrow |e\rangle$  and  $|s\rangle \rightarrow |e\rangle$ ) can interfere and cancel each other, leading to vanishing light absorption in a narrow range of frequencies about the  $|s\rangle \rightarrow |e\rangle$  resonance. [4, 5].

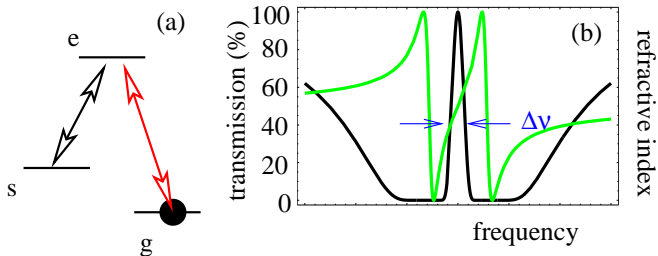


Figure 1: (a) Prototype atomic system for EIT. (b) Spectrum of transmission (black curve) and refractive index (gray curve) corresponding to EIT. Rapid variation of the refractive index causes a reduction of group velocity.

To introduce the idea of a quantum memory let us first consider the case of a pulse of near-resonant light interacting with atoms. Initially this signal pulse is outside the medium in which all atoms are in their ground states ( $|g\rangle$ ). The front edge of the pulse then enters the medium and is rapidly decelerated. Being outside of the medium the back edge still propagates with vacuum speed  $c$ . As a result, upon the entrance into the cell the spatial extent of the pulse is compressed by the ratio  $c/v_g$ , while its peak amplitude remains unchanged. As the pulse exits the medium its spatial extent increases again and the atoms return to their original ground state; the pulse however, is delayed [6] as a whole by

$$\tau = (1/v_g - 1/c)L = \frac{Lg^2N}{c|\Omega|^2}. \quad (1)$$

Inside the medium a wave of flipped spins propagates along with the light pulse. The photons in the pulse are thus strongly coupled to the atoms. We can associate a quasi-particle with this slow propagation, called a dark-state polariton [7]: a combined excitation of photons and spins. If we assume a control field strong enough to be treated classically, we may solve the coupled equations describing the evolution of the signal field and the atomic medium by introducing a new quantum field  $\hat{\Psi}(z, t)$  that is a superposition of photonic and spin-wave (i.e., spin coherence) components:

$$\begin{aligned} \hat{\Psi}(z, t) &= \cos \theta \hat{E}(z, t) - \sin \theta \sqrt{N} \hat{S}(z, t), \\ \cos \theta &= \frac{\Omega}{\sqrt{\Omega^2 + g^2N}}, \quad \sin \theta = \frac{g\sqrt{N}}{\sqrt{\Omega^2 + g^2N}}. \end{aligned} \quad (2)$$

Here  $\hat{E}(z, t)$  is the dimensionless slowly-varying operator representing the signal field, and  $\hat{S}(z, t)$  corresponds to the low-frequency spin-wave.

In the case of ideal spin coherence  $\gamma_{gs} = 0$ , the field  $\hat{\Psi}$  obeys the following equation of motion

$$\left[ \frac{\partial}{\partial t} + c \cos^2 \theta \frac{\partial}{\partial z} \right] \hat{\Psi}(z, t) = 0, \quad (3)$$

which describes a shape-preserving propagation with velocity  $v_g = c \cos^2 \theta$  that is proportional to the magnitude of its photonic component (see [7] for details).

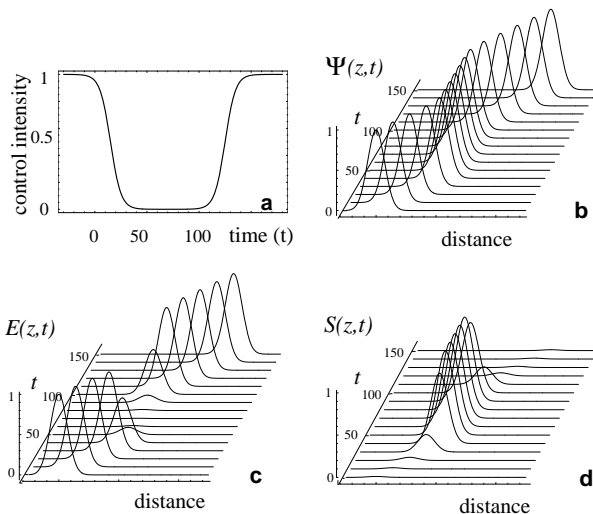


Figure 2: A dark-state polariton can be stopped and re-accelerated by ramping the control field intensity as shown in (a). The coherent amplitudes of the polariton  $\Psi$ , the electric field  $E$  of the signal light pulse and the spin coherence  $S$  are plotted in (b-d).

The quantum memory concept is closely related to that of the dark-state polariton. When a polariton propagates in an EIT medium, it preserves its amplitude and shape, but its properties can be modified simply by changing the intensity of the control beam. As the control intensity is decreased, the group velocity is slowed, and the contribution of photons in the polariton state is reduced, according to Eq. (2). In particular, if the control beam is turned off ( $\Omega(t) \rightarrow 0$ ) the polariton's group velocity is reduced to zero ( $\theta(t) \rightarrow \pi/2$ ) and it becomes purely atomic:

$$\hat{\Psi}(z, t) \rightarrow -\sqrt{N}\hat{S}(z). \quad (4)$$

At this point, the photonic quantum state is mapped onto long-lived spin states of atoms. As long as the mapping process is sufficiently smooth (i.e., adiabatic [8]), the entire procedure has no loss and is completely coherent. The stored quantum state can be easily retrieved by simply re-accelerating the stopped polariton. This is illustrated in Fig. 2 which shows the evolution of the polariton, the signal light pulse, and the spin coherence when the control beam is turned off and on.

The above description is an ideal scenario. In practice the pulse delay is limited by the bandwidth of the transparency window  $\Delta\nu$ , which decreases with propagation distance. This puts a limit on the ratio of delay and pulse duration. The delay can exceed the pulse duration, or in other words, the entire pulse can be localized inside the medium only if an optically dense medium is used, i.e.,  $g^2NL/(c\gamma_{ge}) \gg 1$ . Note that this expression contains the total number of atoms  $N$ , which is a signature of so-called “collective enhancement”. The adiabaticity conditions are analyzed in detail in [9, 10].

Recent experiments have demonstrated some of the light manipulation effects described above by showing that weak pulses can be “trapped” and released after some storage interval [11, 12], and that the storage process is phase coherent [13]. It should be emphasized that all of the experiments carried out so far were in the classical domain, since they involved weak laser pulses in coherent states. An important goal of ongoing work is to apply the light storage technique to quantum states, particularly single photon states, which are most interesting for applications in quantum information.

## 2 Raman Quantum State Manipulation

The above ideas for quantum storage are based on long-lived coherences involving spin states of atomic ensembles, which implies that the interactions between atoms in such states should be sufficiently weak. At the same time, one is naturally interested to develop techniques for non-trivial manipulation of stored quantum states. Such techniques typically involve strong interactions or in other words, large nonlinearity. We now present an example in which a *weakly* nonlinear process (Raman scattering [14]) is used to manipulate atomic quantum states [15, 16]. We then indicate how these ideas can be used to create a robust entanglement of atomic ensembles via realistic (i.e., absorbing) channels.

We again consider a cloud of identical three-level atoms (Fig. 3) that are initially prepared in the ground state  $|g\rangle$ . A sample is excited by an off-resonant laser pulse that induces two-photon Raman transitions into the state  $|s\rangle$ , corresponding to flipped atomic spins that are accompanied by emission of so-called Stokes photons (wavy arrow in the Figure 3). It is important to emphasize that atomic spin flips and Stokes emission events are correlated: for each emitted photon, there is a corresponding flipped spin. We are particularly interested in the forward-scattered Stokes light that is co-propagating with the laser. A photon emitted in this mode is uniquely correlated with the excitation of the symmetric collective spin-wave mode  $S$ , given by  $S \equiv (1/\sqrt{N_a}) \sum_i |g\rangle_i \langle s|$ , where the summation is taken over all the atoms. Specifically, let us assume that the pump pulse duration  $t_p$  is short so that the mean photon number in the forward-scattered Stokes pulse is much smaller than 1. The whole state of the system after the pulse can then be written in the following form

$$|\phi\rangle = |0_a\rangle |0_p\rangle + \sqrt{p_c} S^\dagger a^\dagger |0_a\rangle |0_p\rangle + o(p_c), \quad (5)$$

where  $p_c = 4g^2NL/c|\Omega_p|^2/\Delta^2 t_p$  is the small single-excitation probability and  $o(p_c)$  represents terms with more excitations whose probabilities are  $\leq p_c^2$ . Here  $\Omega_p$  is the Rabi-frequency of the pump field and  $\Delta$  is the single-photon detuning.

Eq. (5) indicates that whenever a single Stokes photon propagating in the forward direction is detected, the state of the atomic ensemble will be given by  $S^\dagger |0_a\rangle$ . That is, the detection of the single Stokes photon “projects” the ensembles into a non-classical state with a single quantum in a well-defined spin-wave mode. Before proceeding, we remark that a large fraction of Stokes light is always emitted in directions other than forward, due to the spontaneous nature of the Raman scattering process. However, whenever the number of atoms  $N$  is large, such events will mostly populate different spin-wave modes, and so the contribution to the population in the symmetric collective mode will be small. As a result, the use of atomic ensembles results in a large signal-to-noise ratio, which enhances the efficiency of the scheme to excite a single-quantum

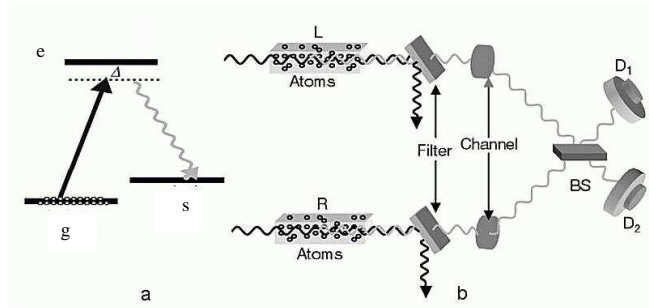


Figure 3: Set-up for probabilistic manipulation of ensemble states. **a.** The relevant level structure of the atoms in the ensemble. **b.** Schematic set-up for generating entanglement between the two atomic ensembles L and R.

spin-wave. The stored spin wave quantum can then be released by conversion into a single-photon wavepacket with well defined properties such as shape and duration.

Such techniques for probabilistic manipulation of atomic ensembles may have an interesting application for long-distance quantum communication in realistic (lossy) photonic channels. As a rule, absorption leads to the exponential loss of signal after propagation over long distances. For example, the degree of entanglement generated by optical means between two distant sites normally decreases exponentially with the length of the connecting channel due to optical absorption and other channel noise. To overcome the difficulty associated with exponential fidelity decay, the concept of “quantum repeaters” can be used [17]. In principle, it allows to achieve an overall quantum state communication fidelity that is very close to unity, with the required resources growing only polynomially with the transmission distance. The basic idea is to divide the transmission channel into many segments, with the length of each segment comparable to the channel attenuation length. First, one generates entanglement and purifies it for each segment; the purified entanglement is then extended to a longer length by connecting two adjacent segments through projective measurement (called entanglement swapping [18]). After entanglement swapping, the overall entanglement is decreased, and one has to purify it again. One can continue the rounds of entanglement swapping and purification until nearly perfect entangled states are created between two distant sites.

There is significant current interest in developing technologies to enable the development and implementation of quantum repeaters. For example, Fig. 3b illustrates how the Raman scattering scheme described above can be used to generate entanglement between two distant atomic ensembles, left (L) and right (R), separated by an absorbing channel [15]. The two pencil-shaped ensembles are illuminated by synchronized classical pump pulses. The resultant forward-scattered Stokes pulses are collected and coupled to optical channels (such as fibers) after polarization- and frequency-selective filtering of the pumping light. The Stokes pulses after the transmission channels interfere at a 50%-50% beam splitter, with the outputs detected respectively by two single-photon detectors  $D_1$  and  $D_2$ . In such a configuration a detector click implies that one quantum of spin excitation has been created in the two ensembles, although it is fundamentally impossible to determine from which of the two ensembles the photon arrived. Thus the single photon measurement projects the state of the system

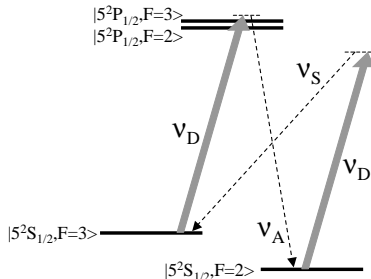


Figure 4: Level scheme for the  $D_1$  line of  $^{85}\text{Rb}$ . A strong drive field (frequency  $\nu_D$ ) induces a four-wave mixing process in which a weak Stokes ( $\nu_S$ ) and Anti-Stokes field ( $\nu_A$ ) are generated.

into an entangled state of two ensembles. This technique can then be extended to implement an entire quantum repeater protocol [15].

### 3 Preliminary Experimental Results

In this section we present preliminary experimental results along the lines outlined above. Specifically, we investigated resonantly enhanced Raman scattering using a warm  $^{85}\text{Rb}$  vapor cell and, with the Raman light, we tested single-photon detection techniques. The latter goal is technologically challenging in the present case, since it requires very sharp optical filtering. The weak Raman signals are co-propagating with pump fields which are typically many orders of magnitude stronger, while the frequency difference between the Raman and pump fields is only a few GHz (3.035 GHz hyperfine splitting for  $^{85}\text{Rb}$ ). Studies of this kind are important in their own right, since the ensemble of Rb atoms forms a strongly non-linear medium in which interesting optical processes occur on a timescale that is much slower than in most nonlinear materials. For example, intensity fluctuations and two-mode photon-number correlations can be slow enough in vapor cell Raman scattering for experimental study with existing photon-count technology (i.e., with nanosecond dead times or longer). The experimental results reported below indicate that the required optical filtering for single-Raman-photon detection can likely be realized, and that photon-count methods can indeed be used to characterize intensity fluctuations in spontaneous, near-resonant Raman scattering.

In our experiments we applied a CW near-resonant pump field to a warm  $^{85}\text{Rb}$  vapor cell ( $T \approx 100$  °C, density  $\approx 10^{12}$   $\text{cm}^{-3}$ ) using an extended-cavity diode laser (power  $P_{in} \approx 5$  mW going into the cell). The cell was contained within three layers of  $\mu$ -metal magnetic shielding. The pump field (frequency  $\nu_D$ ) was applied to the  $D_1$  line, approximately 250 MHz blue-detuned from the center of the Doppler-broadened  $5^2S_{1/2}, F = 3 \rightarrow 5^2P_{1/2}, F = 3$  transition (see also Fig. 4). The pump field induced a CW four-wave-mixing process, under conditions of electromagnetically induced transparency (EIT), as indicated in Fig. 4. In this scheme the same pump field coupled both the  $F = 2$  and the  $F = 3$  ground states to the excited states. Using a

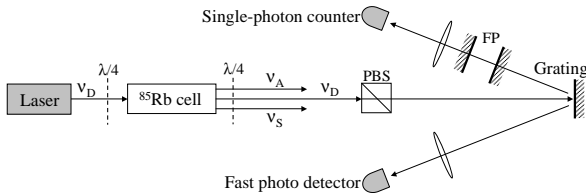


Figure 5: Schematic of the Raman-statistics experimental setup with Fabry-Perot (FP) and polarizing beam splitter (PBS).

Fabry-Perot interferometer, we observed the residual transmitted pump field, as well as Raman Stokes ( $\nu_S$ ) and anti-Stokes fields ( $\nu_A$ ), which predominantly propagated collinearly with the pump beam (the power in the Raman fields was at most 10 - 100  $\mu\text{W}$ ). To study the quantum statistical properties of these spontaneously generated fields, it was crucial to isolate effective single modes via polarization, frequency, and spatial mode filtering. This was implemented with the setup shown in Fig. 5, using a Fabry-Perot etalon and a polarizing beam-splitter. Additionally, we used a diffraction grating, and (not shown) interference and color filters as well as pinholes: (i) to suppress contributions from the spontaneous emission background of the laser; and (ii) to allow for simultaneous detection with single-photon-counters and fast photo detectors (for time-resolved detection of fluctuations or recording the spectrum of beat note signals). With the cell length  $L = 7$  cm and a beam diameter  $D \approx 1$  mm, the Fresnel number  $D^2/\lambda L$  was somewhat larger than 1. Nevertheless, our results indicate that it is feasible to detect signals from a single spatial mode, possibly due to wave-guiding effects induced by the strong pump field in the near-resonant vapor.

The observed power of the Raman fields  $\nu_S$  and  $\nu_A$  showed a threshold-like behavior as a function of the input pump field power  $P_{in}$  (Fig. 6), and pump detuning. Photon count studies of the spontaneous Stokes and anti-Stokes fields below threshold indicated statistics that approached Bose-Einstein behavior (i.e., thermal statistics, which are characteristic for fields from spontaneous processes). For example, Fig. 7 shows histograms from photon-count measurements with 500 ns count windows. Studies of the beat note signal at  $\nu_D - \nu_S$  offset from the co-propagating pump and Raman fields gave a linewidth of  $\Delta\nu_B \approx 500$  kHz (limited by atom transit time through the beam). This result indicates that the count-window values we used were shorter than  $1/\Delta\nu_B$ , which is required for effectively probing a single spectral mode. The observation of near-Bose-Einstein statistics below threshold (i.e., at low  $P_{in}$ ) confirms that we indeed selected a single Raman mode, since the photon statistics that results from detecting multiple thermal modes converges very rapidly to a Poisson distribution [19].

When increasing the pump power  $P_{in}$  to above threshold (Fig. 6), we observed that the photon count statistics crossed over from Bose-Einstein to Poisson statistics (Fig. 7). For photon counting with stronger Raman fields, we used 10 - 20 dB of attenuation to prevent detector saturation. While such attenuation can in general alter the measured photon statistics, counting results from slow thermal fluctuations are robust against moderate losses, and we believe the added attenuation was not responsible for the observed crossover to Poisson statistics. The Bose-Einstein to Poisson crossover could be due to the fact that the increase of  $P_{in}$  causes a change

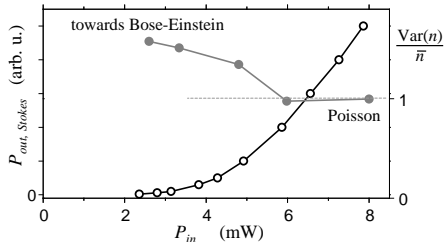


Figure 6: Threshold behavior of the power of the generated output Stokes field vs. the power of the input pump field  $P_{in}$  (open circles). At the higher values of  $P_{in}$  the photon-count results have Poisson statistics, with values of  $Var(n)/\bar{n} \approx 1$  (solid circles, right axis). For lower  $P_{in}$  values the fluctuations in the Stokes field are larger, and approach Bose-Einstein statistics. See also Fig. 7.

from a single mode to a multiple mode measurement. However, at larger  $P_{in}$  the width of the beat note signal  $\Delta\nu_B$  did not broaden beyond the inverse counting time. Also, checks on the efficiency of the filtering system did not show a significant dependence on  $P_{in}$ . Therefore, we believe that the results at higher  $P_{in}$  still correspond to detection of a single spectral mode. We also checked that the beam profiles of the transmitted fields did not change significantly as  $P_{in}$  varied, so there was no indication of a crossover to probing multiple spatial modes.

Thus we conclude that the crossover to Poisson statistics is likely caused by a fundamental process corresponding to a transition from spontaneous to stimulated Raman scattering in the cell [20, 21]. However it is remarkable that in the case of near-resonant excitation the crossover occurs at low Raman conversion efficiencies; the origin of this unexpected behaviour is not at present well understood.

With our detection method, we observed that the depleted pump field transmitted through the cell can develop noise properties similar to those of the Raman fields. In fact, depending on the pump power and detuning, we could realize all combinations with either Poisson or near-Bose-Einstein count statistics for the residual pump field, and Poisson or near-Bose-Einstein count statistics for the Stokes field. The striking enhancement of noise on the residual pump light is best illustrated with the results presented in Fig. 8. This figure shows Fabry-Perot scans across the transmission resonance for (a) the Stokes field and (b) the residual pump field. When the Raman process is effective, we observed a noisy transmission resonance for the Stokes mode and the residual pump field, both fields had near-Bose-Einstein statistics. However, when the Raman process in the cell was suppressed with a magnetic field, the noise on the residual pump transmission dropped to the level of detector noise. This field then had Poisson statistics, as expected for a field from a coherent source.

A particular feature of the Raman-induced noise on the residual pump field is that the fluctuations can be as large as the average output intensity of the residual pump field. A second observation is that under these conditions the output pump field has a power similar to that of the Raman fields, indicating that in this regime a non-linear attenuation of the pump field can no longer be neglected. We believe that the origin of this behaviour is a so-called pulse matching effect [22]. Due to nonlinear conversion,



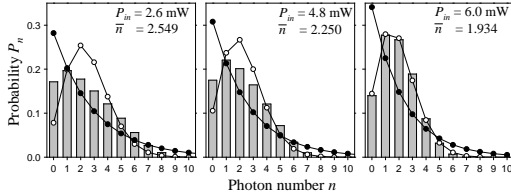


Figure 7: Histograms of Stokes field photon-count results for different values of pump power  $P_{in}$ . Results are for 500 ns count windows. Gray bars are experimental results. For comparison, curves for Bose-Einstein statistics (solid circles) and Poisson statistics (open circles) are plotted for the experimental value of the mean photon count  $\bar{n}$ .

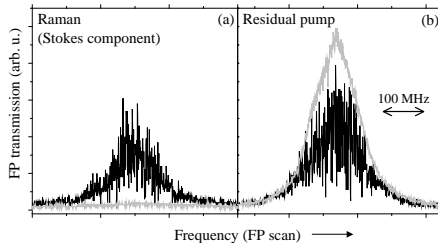


Figure 8: Transmission signals from Fabry-Perot scans show noise on (a) the Stokes field, and (b) the residual pump field (black trace). When Raman scattering is suppressed with a magnetic field the noise on the pump field vanishes (gray trace).

the pump field is attenuated until the two pairs of fields in Fig. 4 match intensities in such a way that the atoms evolve into a common EIT-like dark state [23]. Under these conditions the atoms force a matching of all field fluctuations, and the noise properties of the Raman fields are mirrored in the transmitted pump intensity.

In summary, our preliminary experiments indicate that quantum statistical properties of near-resonant Raman fields can be studied with photon-counting methods. In particular, we observed a crossover between Bose-Einstein and Poisson statistics and showed that the noise properties of Raman fields can be mirrored in transmitted pump beams. However, observation of significant quantum correlations will require low and well-characterized losses, as well as improvements in the filtering system – problems which are currently under investigation.

## 4 Acknowledgments

The theoretical ideas described here were developed in on-going collaboration with J. I. Cirac, L. M. Duan, M. Fleischhauer, S. Yelin and P. Zoller. It is our pleasure to thank them for many useful interactions. We are also grateful to T. P. Zibrova for

assistance with semiconductor lasers and to R. Glauber for many useful discussions. This work is supported by NSF ITR program, DARPA and ONR. Partial support by NASA and MIT-Harvard CUA is also acknowledged. CHW acknowledges support from a fellowship through the Netherlands Organization for Scientific Research (NWO). MDE acknowledges support from a National Science Foundation Graduate Research Fellowship.

## References

- [1] J. I. Cirac, P. Zoller, H. Mabuchi, and H. J. Kimble, *Phys. Rev. Lett.* **78**, 3221 (1997).
- [2] S. E. Harris, *Phys. Today* **50**, 36 (1997).
- [3] M. D. Lukin and A. Imamoglu, *Nature* **413**, 273 (2001).
- [4] E. Arimondo, in *Progress in Optics*, ed. E. Wolf, North-Holland, Amsterdam, Vol. **35**, p. 259 (1996).
- [5] K. Boller, A. Imamoglu, and S. E. Harris, *Phys. Rev. Lett.* **66**, 2593 (1991).
- [6] S. E. Harris, J. E. Field, and A. Kasapi, *Phys. Rev. A* **46**, R29 (1992).
- [7] M. Fleischhauer and M. D. Lukin, *Phys. Rev. Lett.* **84**, 5094 (2000).
- [8] J. Oreg, F. T. Hioe, and J. H. Eberly, *Phys. Rev. A* **29**, 690 (1984).
- [9] A. B. Matsko *et al.*, *Adv. At. Mol. Phys.* **46**, 191 (2001).
- [10] M. Fleischhauer and M. D. Lukin, *Phys. Rev. A.* **64**, 022314 (2002).
- [11] C. Liu., Z. Dutton, C. H. Behroozi, and L. V. Hau, *Nature* **409**, 490 (2001).
- [12] D. F. Phillips, M. Fleischhauer, A. Mair, R. L. Walsworth, and M. D. Lukin, *Phys. Rev. Lett.* **86**, 783 (2001).
- [13] A. Mair, J. Hager, D. F. Phillips, R. L. Walsworth, and M. D. Lukin, *Phys. Rev. A* **65**, 031802 (2002).
- [14] M. G. Raymer, I. A. Walmsley, J. Mostowski, and B. Sobolewska, *Phys. Rev. A* **32**, 332 (1985).
- [15] L. M. Duan, M. D. Lukin, J. I. Cirac, and P. Zoller, *Nature* **414**, 413 (2001).
- [16] A. André, L. M. Duan, and M. D. Lukin, *Phys. Rev. Lett.* **88**, 243602 (2002).
- [17] H. J. Briegel, W. Duer, J. I. Cirac, and P. Zoller, *Phys. Rev. Lett.* **81**, 5932 (1991).
- [18] M. Zukowski, A. Zeilinger, M. A. Horne, and A. Ekert, *Phys. Rev. Lett.* **71**, 4287 (1993).
- [19] L. Mandel and E. Wolf, *Optical Coherence and Quantum Optics*, Cambridge Univ. Press, Cambridge (1995).
- [20] A. S. Grabchikov, S. Ya. Kilin, V. P. Kozich, and N. M. Iodo, *JETP Lett.* **43**, 151 (1986).
- [21] P. A. Apanasevich, D. E. Gakhovich, A. S. Grabchikov, S. Ya. Kilin, V. P. Kozich, B. L. Kontsevoi, and V. A. Orlovich, *Sov. J. Quantum Electron.* **22**(9), 822 (1992).
- [22] S. E. Harris, *Phys. Rev. Lett.* **70**, 552 (1993).
- [23] M. D. Lukin, P. R. Hemmer, M. Löffler, and M. O. Scully, *Phys. Rev. Lett.* **81**, 2675 (1999).